Challenge Journal of CONCRETE RESEARCH LETTERS

Research Article

Utilization of fly dust generated during fired shale production for the preparation of aggregates and geopolymers

Jan Urbánek [a,*], Petr Antoš [b]

[a] *Technopark Kralupy, University of Chemistry and Technology Prague, 27801 Kralupy nad Vltavou, Czechia*

ABSTRACT

Fly shale dust (FSD) is a fine secondary powder that is produced during the firing of shales in a rotary kiln. Its use is relatively limited, and therefore it is usually landfilled, despite its chemical composition being similar to chamotte. The main challenge is the wide firing temperature range. As a result, the material partially retains plastic properties and at the same time contains high-temperature phases. The second challenge is the significant fineness of the material, which makes it impossible to burn it in a rotary kiln. To evaluate its suitability, FSD powder was granulated with water and subsequently fired at temperatures ranging from 800 °C to 1650 °C to produce a refractory aggregate. Analysis of the high-temperature product confirmed a high mullite content and low porosity, as well as high refractoriness, which was further improved by the addition of alumina. The next part of the work was focused on the use of FSD for metakaolin production, where granulated material was calcined at 600-850 °C. The sample with the highest pozzolanic activity was selected for geopolymer preparation. Potassium or sodium water glass was used as the activator, blast furnace slag or cement as the hardener, and chamotte aggregate as the filler. The obtained material reached the compressive strength of concrete class C60/75. The results provided important information about the key steps of FSD processing and confirmed its potential for practical application.

ARTICLE INFO

Article history:
Received – November 7, 2025
Revision requested – December 24, 2025
Revision received – January 26, 2026
Accepted – February 1, 2026

Keywords:
Fly dust
Shale
Clay
Aggregate
Geopolymer

Citation: Urbánek J, Antoš P (2026). Utilization of fly dust generated during fired shale production for the preparation of aggregates and geopolymers. *Challenge Journal of Concrete Research Letters*, 17(1), 71–81.

1. Introduction

Formerly, chamber furnaces and charcoal piles were used for fireclay production. These technologies are now considered inadequate and have been displaced by the rotary kiln (Boateng 2008). Among the main advantages of rotary kilns are the possibility of automation, uniform continuous firing, and material processing in a wide range of fractions, high feed capacity and high operational temperatures (Bojanovský et al. 2022). During firing, flue gases are produced, which are blown out of the furnace by a connected fan. Blowing out also provides a slight underpressure in the furnace, which is critical for its safe and stable conditions (Zheng et al. 2022). Along with the flue gases, fine fly clay dust is carried away from the furnace and subsequently captured on collectors (Abdelgader et al. 2022). Due to the extremely high temperatures in the rotary kiln and the low temperature resistance of the filter material (up to 250 °C), the output mixture must be quickly cooled, for example, by using an auxiliary fan or a heat exchanger. At the same time, a multi-stage thermal filter protection system is used. The last protection is a short-term bypass switch directly to the fan. The obtained fly clay dust is characterized by high fineness and non-uniform properties. Its utilization is typically very limited. Therefore, it is usually landfilled. The production of aggregates, fillers and binders represents one of the potential methods for its effective reuse (Özkılıç et al. 2023; Lam et al. 2021; Jala and Sharma 2019; Riaz et al. 2022;

* *Corresponding author*. E-mail address: urbanekj@vscht.cz (J. Urbánek)
ISSN: 2548-0928 / DOI: https://doi.org/10.20528/cjcrl.2026.01.006

Padmalosan et al. 2023; Kaminskas and Savickaite 2023; Saleh et al. 2021).

Shale is a laminated or fissile claystone (Sheng 2020). It is a sedimentary rock formed by the settling of clay particles with a moderately consolidated layered structure with a particle size below 63 μm (Rimstidt et al. 2017; Muhammed et al. 2021). Shales consist mainly of clay minerals, predominantly kaolinite and also contain quartz, feldspar, iron oxides, carbonates, coal etc. (Aird 2019). They are processed by firing at temperatures of approximately 1350 °C to form refractory fireclay (Djangang et al. 2008). Fired shales are characterized by volume stability and good resistance to thermal shock. They are used in power generation blast furnaces, chimney linings, boilers, glass tank furnaces and pottery kilns (Debnath et al. 2022). The quality of fireclay is evaluated based on the amount of mullite and its degree of densification (Malaiškiene et al. 2022).

Due to its high kaolinite content, shale can also be used for the production of metakaolin. Metakaolin is an amorphous aluminosilicate that is a highly reactive natural pozzolan produced by the calcination and dehydroxylation of kaolinitic clay at temperatures between 500 °C and 900 °C (Panesar 2019; Provis and Bernal 2014). Depending on the origin of the raw materials, the chemical composition might vary (Bucher et al. 2021). Metakaolin is used as a cement replacement in concrete, leading to improved durability and a reduced environmental impact associated with the cement industry (Rasekh et al. 2020; Pillay et al. 2021). Metakaolin is rather expensive (Lopes et al. 2023) and therefore its production remains limited. Another application of metakaolin is as a precursor for geopolymer production (Aziz et al. 2015). The process involves the dissolution of the aluminosilicate source material in an alkaline solution (alkaline activator) to form aluminate-silicate hydrates, followed by a condensation reaction and subsequent hardening. Geopolymers exhibit excellent mechanical properties, durability, acid resistance and high temperature stability (Cong and Cheng 2021).

The aim of this study is to evaluate the reuse potential and application possibilities of fine fly shale dust (FSD) in construction materials. The work investigates the large-scale thermal treatment of powdered FSD, including firing to produce refractory aggregate and calcination to obtain reactive metakaolin. Key properties affecting applicability, such as refractoriness and pozzolanic activity, are evaluated. In the case of metakaolin, geopolymer binders are prepared and their mechanical properties are compared with literature data. In contrast to most previous studies, which focus on a single utilisation route, this work demonstrates a dual, construction-oriented valorisation of FSD using industrially applicable processes, including granulation, drying, firing, and grinding, which are commonly available in facilities engaged in clay processing and firing.

2. Materials and Methods

The fine fly shale dust (FSD) was obtained from České lupkové závody, a company specializing in the mining, firing and granulometric processing of refractory clays. The powder contained particles in the size range of 0-500 μm, with d_{60} being 31 μm and d_{90} being 123 μm. It contained a large amount of Al_2O_3 and a relatively low proportion of melting oxides (Table 1). The chemical composition may vary depending on the deposit location; for example, the Fe2O3 content ranges from 1.25% to 3.8%. A similar situation is observed for the mineralogical composition, which is additionally influenced by the firing temperature. Of the crystalline phases, it contained kaolinite, mica in the form of muscovite, quartz, anatase and high-temperature phases mullite and cristobalite (Table 2). Considering the relatively high proportion of mullite, it is clear that part of the material was exposed to high temperatures above 1050 °C. Furthermore, spherical ash particles were registered. They originate from powdered coal, which is used to heat the rotary kiln. SEM/EDS analysis showed that the chemical composition of individual particles varies in the content of minor fluxing oxides (K_2O, CaO, Fe_2O_3), particularly among spherical ash particles. In order to understand the processes during the firing, a thermal analysis of the FSD was carried out.

Table 1. Chemical composition of raw materials. (The contents are given in weight percent, normalized to 100%.)

Title	Al_2O_3	SiO_2	Fe_2O_3	TiO_2	Na_2O	K_2O	CaO	MgO
FSD	44.15	48.26	2.11	2.29	0.21	0.88	0.83	0.33
Kaolin	43.31	53.18	0.64	1.00	0.07	1.32	0.07	0.15
Alumina	99.35	0.18	0.05	–	0.15	0.05	0.02	0.13

Table 2. Mineralogical composition of FSD. (The contents are semiquantitative and expressed in weight percent, normalized to 100%. The sample contains a significant amount of amorphous phase.)

Title	Kaolinite	Mullite	Muscovite	Quartz	Anatase	Cristobalite
FSD	41	30	17	8	2	2

In the experimental work, the possibilities of using a commercial sample of FSD for the production of refractory aggregates were tested. The FSD was first mixed and homogenized with water in a ratio of 4:1 and granulated using an extruder equipped with a mesh adapter with an outlet mesh diameter of 9 mm (Fig. 1). The granules were dried at 110 °C to a constant weight and after cooling, were sieved manually using sieves 1.25, 2.5, 5.0, 7.1 and 10 mm. The 7.1-10 mm fraction was used for further analyses.

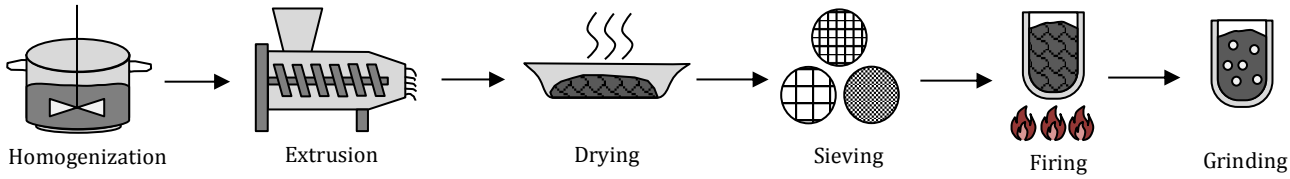

Fig. 1. Process scheme.

80-100 g of granulate was placed into a corundum crucible, which was fired in an electric furnace at temperatures of 800, 1150, 1250, 1350, 1450, 1550 and 1650 °C. Heating was performed at 5 °C/min, with a 3 h dwell time, followed by free cooling. Based on the weight loss, the loss on ignition was determined. The density criteria (bulk density, apparent porosity, absorbency) were determined by soaking the granules under vacuum in water. The soaking procedure was based on the EN 993-1 (2018) standard, while the granules were weighed on a steel sieve under water. Part of the fired granules was ground in a planetary mill. The resulting powder was used for analysis of phase composition using X-ray diffraction and particle morphology using electron microscopy. To increase the strength of the granules after drying, the effect of the addition of kaolin was tested. Furthermore, to increase the refractory properties, the influence of the addition of alumina (FEPA size: F-1200) was tested. The composition of the mixtures is shown in Table 3. With regard to the different absorbency of the individual components, the amount of added water was adjusted so that the mixtures exhibited similar plasticity after mixing.

Table 3. Composition of mixtures for granulate production.

Title	Content (%)			
	FSD	Kaolin	Alumina	Water
R	100	-	-	25
RK	80	20	-	28
RA	67	-	33	23

The chemical composition of the raw materials is given in Table 1. Rods from all three mixtures were prepared by manual tamping into molds with a size of 40×40×160 mm. After 24 hours, the samples were unmolded and dried in an oven at a gradually increasing temperature up to 110 °C. After cooling, the samples were cut into 4 cm cubes and their compressive strength was determined. Cylindrical samples were prepared from the mixtures in a similar way for analysis of refractoriness under load according to the EN ISO 1893 standard. The samples were then pre-fired at a temperature of 1350 °C.

The second research direction involved testing the potential use of FSD for the production of metakaolin. Dried granules from mixture R, prepared according to the above procedure, were fired at a rate of 5 °C/min at temperatures of 600-850 °C with a duration of 3 hours. After cooling, the granulate was ground in a planetary mill at 400 rpm for 30 min. The resulting powder was used to determine the pozzolanic activity using the Chapelle test. The principle of the method is heating and homogenizing a mixture consisting of 0.33-0.34 g of the sample, 0.43-0.44 g of CaO and 80 ml of distilled water at 93 °C for 17 hours. After cooling and filtering, the content of dissolved calcium in the filtrate is determined by titration with 0.1M HCl. The result of the measurement is a number indicating the amount of $Ca(OH)_2$ bound by one gram of pozzolan, i.e. the analyzed sample. The sample fired at 650 °C with the highest pozzolanic activity ($FSD_{650°C}$) was further used to verify the possibility of its application for the production of geopolymers. They consisted of the following components. Potassium water glass (PWG) with a modulus of 1.7 and sodium water glass (SWG) with a modulus of 2.0 were used as activators, slag and alumina cement Górkal 40 as a hardener, a commercial silicone-based sample as a plasticizer and chamotte aggregate A111 with a grain size of 0-1 mm as a filler. A complete overview of the composition of the tested geopolymer mixtures is given in Table 4. The formulations of the mixtures were based on patents US20160152521 and US2010010139A, which relate to the use of the pozzolanic activity of fly ash. The water content of the MPSl and MefPSl samples was adjusted to achieve a vibroplastic consistency.

The mixtures were homogenized using a planetary mixer and then manually or vibro-tamped into molds with dimensions of 40×40×160 mm. The setting was carried out according to the following procedure. The samples were covered with plastic wrap to prevent significant drying and left for 24 hours in the molds at room temperature. Subsequently, they were unmolded and placed on wire racks for another 24 hours and finally hardened in an oven at 60 °C. The resulting rods were used to determine the flexural strength, compressive strength and density criteria. For the selected mixtures, the refractoriness under load was also determined. To compare the quality of metakaolin prepared from FSD, a geopolymer sample was also prepared from commercial metakaolin Mefisto L05, and its properties were subsequently analyzed.

Table 4. Composition of geopolymer samples. (FSD650°C – fly shale dust fired at 650 °C, PWG – potassium water glass, SWS – sodium water glass, cement. The water content is expressed relative to 100% of the remaining mixture.)

Sample	Metakaolin (%)		Activator (%)		Hardener (%)		Water (%)	Filler (%)	
MPSl	$FSD_{650°C}$	64.9	PWG 1.7	18.9	Slag	16,2	14,0	-	-
MefPSl	$Mefisto_{L05}$	64.9	PWG 1.7	18.9	Slag	16,2	20,3	-	-
MPSlCh	$FSD_{650°C}$	16.9	PWG 1.7	13.5	Slag	3.0	-	Chamotte	66.7
MSSlCh	$FSD_{650°C}$	16.9	SWG 2.0	13.5	Slag	3.0	-	Chamotte	66.7
MSCCh	$FSD_{650°C}$	16.9	SWG 2.0	13.5	Cement	3.0	-	Chamotte	66.7

3. Results and Discussion

3.1. Aggregates

In order to granulate the mixture of FSD with water or with other raw materials, a relatively narrow range of water content had to be used. If the water content was too low, the mixture was insufficiently plastic and it was not possible to push it through the output adapter of the extruder (Salehi and Salem 2008). With an excess of water, long fibers were formed, which stuck together to form a compact mass. Under optimal conditions, elongated cylindrical granules were formed, which contained numerous cracks due to the excess solid phase and relatively high output pressure. During handling of dried granules (for example, during manual sieving) they broke at the place of cracks into smaller cylindrical and spherical particles (Fig. 2). The content of fine particles below 1.25 mm was 22%.

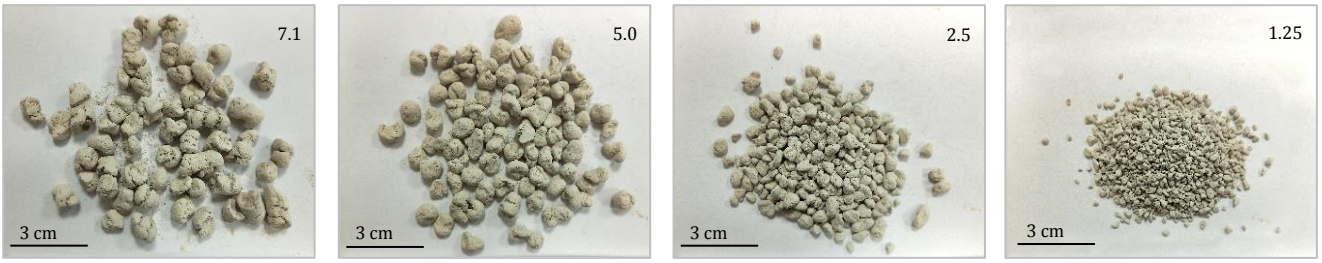

Fig. 2. Granulate fraction on sieve 7.1, 5.0, 2.5, and 1.25 mm.

The granules were relatively strong. It was difficult to squeeze them between the fingers. They exhibited low abrasion resistance, as also evidenced by the relatively high proportion of fine particles. The compressive strength after drying of the manually tamped samples was around 1 MPa for all three tested mixtures R, RK and RA. Their bulk density reached 1550-1600 kg/m^3, in the case of the mixture with alumina almost 1800 kg/m^3. Loss on ignition of granules after firing at a temperature of 1150 °C reached 6.2% (R), 7.0% (RK) and 3.9% (RA). The mixture with alumina showed a lower loss due to its lower clay content, and consequently a lower proportion of chemically bound water. The progression of granule sintering is shown in the graphs in Fig. 3. Samples R and RK exhibited a relatively similar behavior. Their more pronounced sintering occurred in the temperature range of approximately 1150-1450 °C. After firing at 1450 °C, they showed a bulk density of approximately 2180 kg/m^3, an absorbency of 4.1% and an apparent porosity of 9.0%. In the case of the mixture RA, more pronounced sintering occurred at 200-250 °C higher compared to the other two samples. After firing at 1650 °C, it had a bulk density of 2290 kg/m^3, an absorbency of 6.8% and an apparent porosity of 15.6%.

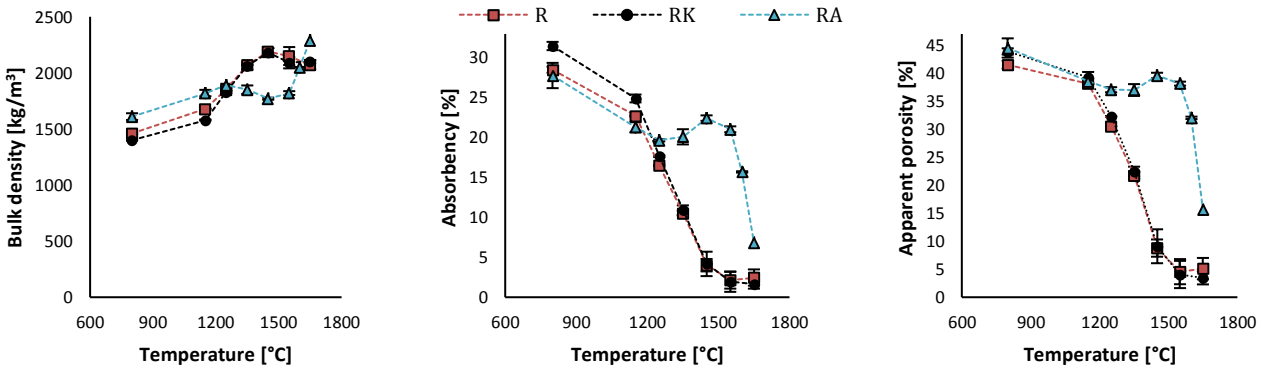

Fig. 3. Dependence of bulk density, absorbency and apparent porosity of granulate on firing temperature. (number of measurements: n = 3)

The results of the thermal and mineralogical analysis of the FSD and the granules R and RA made from it are shown in the graphs in Figs. 4 and 5. In the temperature range up to approximately 200 °C, free water was removed corresponding to a 0.58% weight loss. The majority weight loss of 5.4% was registered in the temperature interval of about 450-650 °C, with a maximum at 540 °C associated with the dehydroxylation of kaolinite. Dehydroxylation of muscovite occurred in the temperature range of approximately 700-900 °C, with a maximum at about 850 °C (Jia, et al. 2015). The interpretation of the exothermic band at a temperature of 978 °C is not unequivocal. It included theories such as the formation of γ-Al_2O_3, Al-Si spinel, mullite or SiO_2. In more detail, the whole subject is discussed in the book Phase Transformation of Kaolinite Clay (Chakraborty 2014). At temperatures above 1050 °C, the formation of high-temperature phases mainly mullite and cristobalite occurred, while the quartz content decreased. Above 1350 °C, the cristobalite content decreased, while the mullite fraction further increased. The total loss of ignition after firing at 1400 °C was 6.70%. The addition of alumina led to a higher mullitization of the aggregates after firing above 1350 °C. A side effect of the reaction was a reduction, to nearly zero, of the cristobalite fraction compared to FSD alone. Mullite, formed by needle-shaped crystals, is characterized by high refractoriness above 1700 °C and a low coefficient of thermal expansion 4.5–5.6 × 10^{-6} K^{-1} (Samadi et al. 2022), thereby contributing to enhanced mechanical strength, refractoriness – as confirmed by the graph in Fig. 7, and resistance to sudden temperature changes. Given its relatively low content, cristobalite is not expected to significantly affect the properties of fired FSD. At higher contents, however, microcracks and a reduction in strength may occur due to the α ↔ β phase transformation at approximately 220 °C, which is accompanied by a ~5% volume change (Stokes 2024).

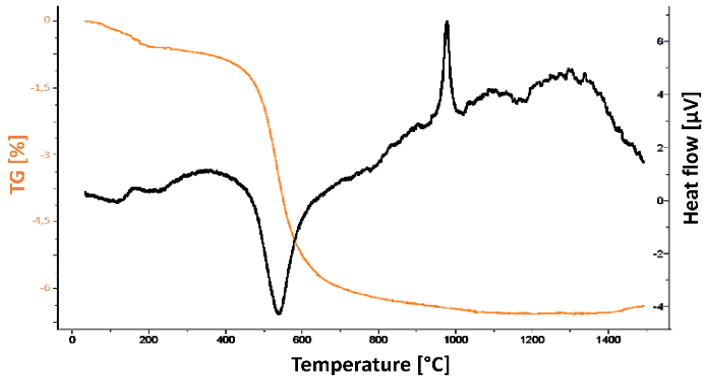

Fig. 4. TG-DTA analysis of the FSD. (weight 65.11 mg, rate 5 °C/min, atmosphere air)

Electron microscope photographs of the FSD and ground granules R fired at temperatures of 650, 1350 and 1650 °C are shown in Fig. 6. Spherical ash particles were visible in the FSD. Partial sintering was observed on the surfaces of granules fired at 1350 °C. After firing at 1650 °C, complete sintering occurred. In the corresponding photo, larger sharp-edged particles of the aggregates were visible, accompanied by finer particles formed during the grinding of the granulate.

The results of the refractoriness under load analysis of the samples R, RK and RA are shown in the graphs in Fig. 7 (graphs a and b). In the case of the unfired sample R, deflection occurred at a significantly lower temperature compared to the sample fired at 1350 °C. The deflection was not caused by lower refractory properties, but by shrinkage resulting from sintering and phase transformations. The refractory properties of samples R and RK were partly similar. Their more significant deformation during the heat resistance test occurred at temperatures above 1350 °C, likely due to shrinkage, among other factors. The addition of alumina increased the deformation temperature (Andrews et al. 2013), in the case of the RA sample by about 100 °C.

3.2. Metakaolin

A commercial sample of metakaolin, designated Mefisto L05, had a pozzolanic activity of 932 mg/g. The FSD exhibited a low pozzolanic activity of 172 mg/g. Firing in the temperature range of 600-850 °C increased its pozzolanic activity (Fig. 8) with a maximum value of 476 mg/g observed after firing at 650 °C. This was in accordance with the results of the thermal analysis, which indicated that the dehydroxylation of kaolinite occurs in the temperature range of 500–650 °C. Commercial metakaolin contained very fine particles with d_{50} = 3 µm and d_{90} = 10 µm, while metakaolin prepared from FSD contained coarser particles. This was attributed to the lower efficiency of the planetary mill used to grind the fired granulate. No significant increase in pozzolanic activity was observed when the grinding time was extended beyond 30 minutes. The same trend was observed for the fraction below 32 µm. By grinding metakaolin to a finer particle size, or to a size comparable to the commercial sample, an increase in its pozzolanic activity could be expected. However, FSD cannot achieve the pozzolanic activity of the commercial sample because it has already been partially exposed to high temperatures during industrial processing, resulting in the conversion of part of the original kaolin into high-temperature phases, primarily mullite, as evidenced by the diffractogram in Fig. 5.

The fired sample of metakaolin, like the original FSD, partially contained high-temperature phases. As a result, it showed a lower absorbency compared to the commercial sample. Its oil number was 36 g/100 g, while the Mefisto L05 exhibited 51 g/100 g. The difference in absorbency had to be considered when preparing geopolymer samples with regard to the desired consistency of the mixture.

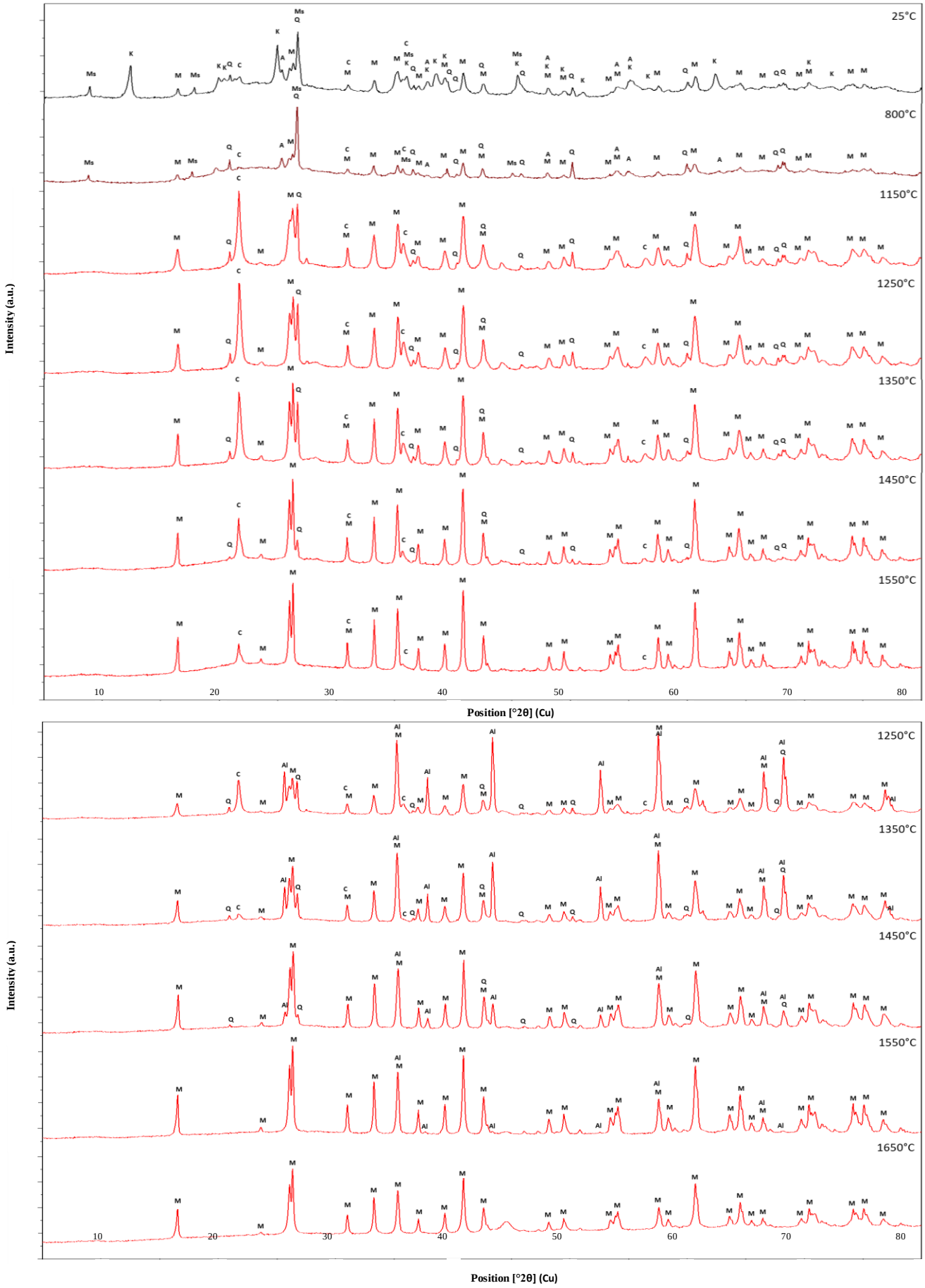

Fig. 5. Diffractogram of granulate R (top) and RA (bottom) depending on firing temperature. (M – mullite, Q – quartz, C – cristobalite, K – kaolinite, Ms – muscovite, A – anatase, Al – corundum)

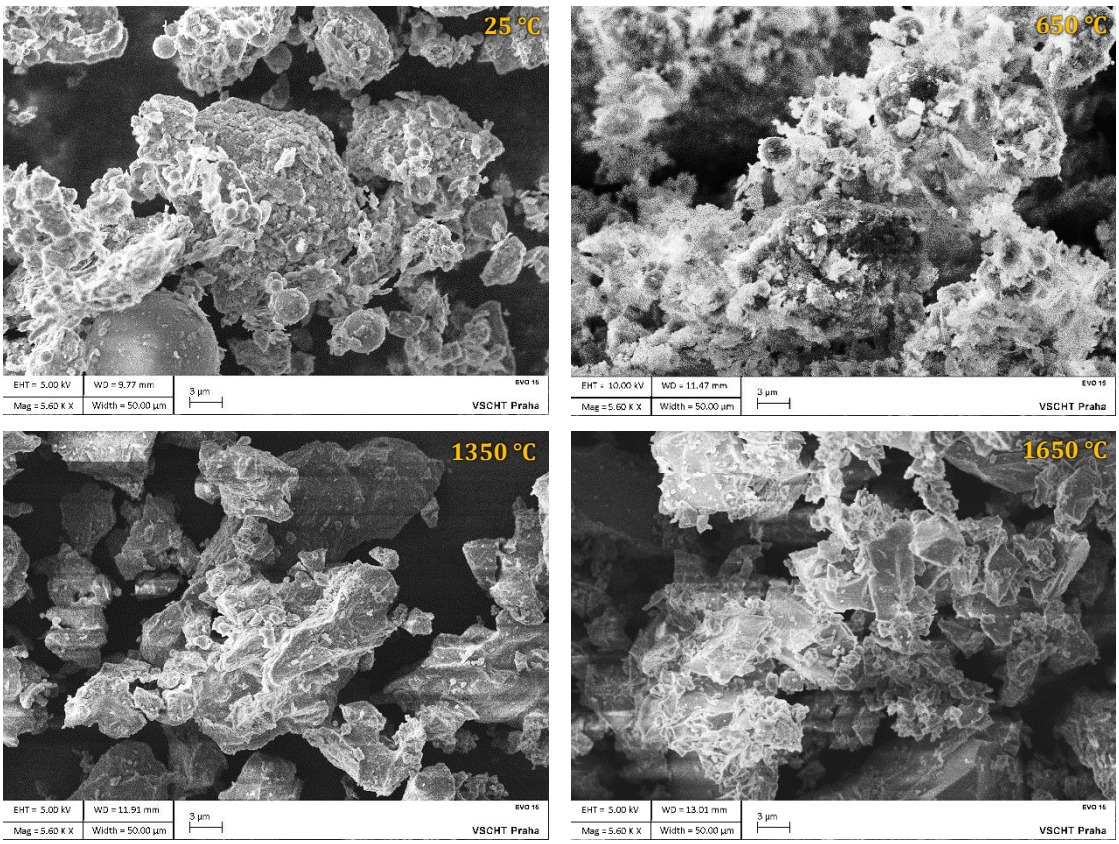

Fig. 6. Photos of original FSD and fired at temperatures of 650, 1350 and 1650 °C.

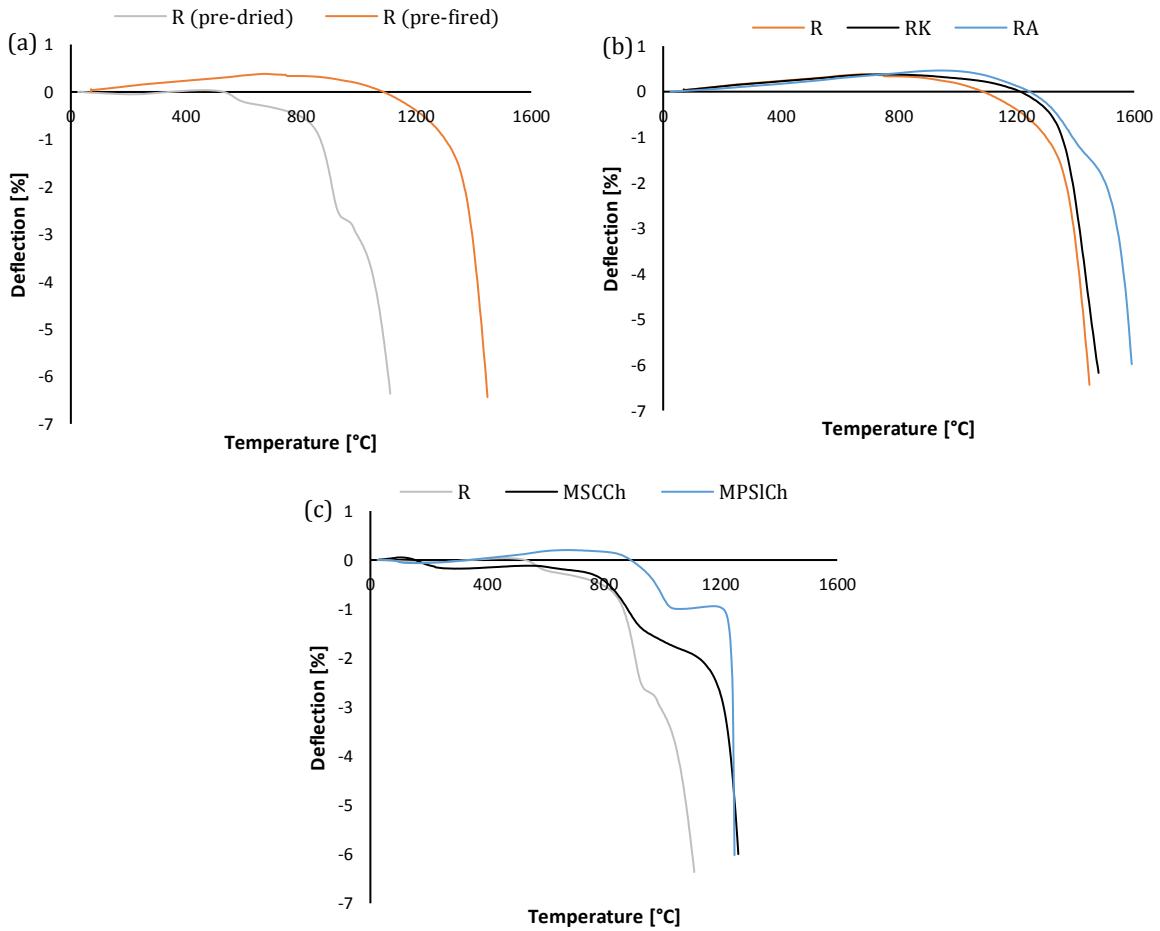

Fig. 7. Refractoriness under load: (a) Sample R pre-dried at 110 °C and the pre-fired at 1350 °C; (b) Samples R, RK and RA pre-fired at 1350 °C; (c) MSCCh and MPSlCh geopolymer samples R pre-dried at 60 °C and for comparison sample R pre-dried at 110 °C.

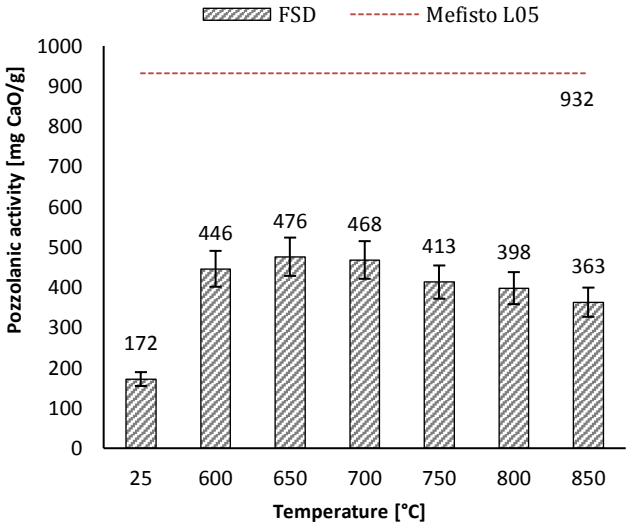

Fig. 8. Dependence of pozzolanic activity of FSD on firing temperature. (According to AFNOR (2012), the results are expected to fall within a ±10% variation.)

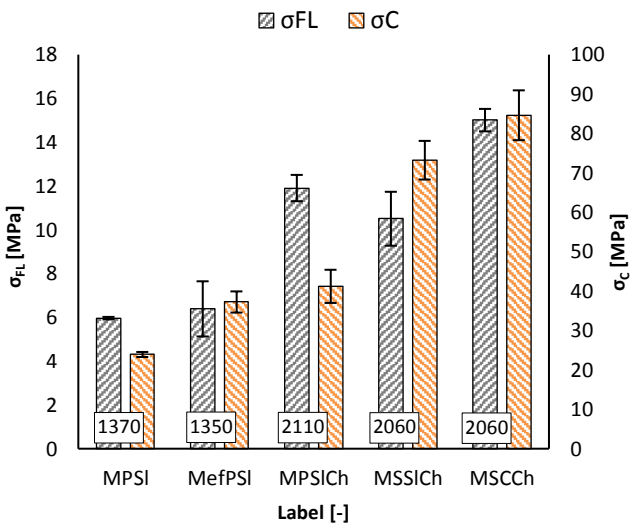

Fig. 9. Flexural and compressive strength and bulk density (at the base) of geopolymer samples (n = 3; 4).

Test samples of geopolymers MPSl and MefPSl exhibited vibroplastic consistency. Samples with the addition of chamotte aggregate MPSlCh, MSSlCh and MSCCh showed a ramming consistency. Geopolymers were prone to cracking due to shrinkage during setting and hardening (Khan et al. 2019). Cracks usually did not occur in samples containing filler due to an excess of aggregates. The mechanical properties of the samples are shown in Fig. 9. Geopolymers from prepared and commercial metakaolin MPSl and MefPSl showed similar flexural strength of approx. 6-6.5 MPa, but a different compressive strength of 24 MPa compared to 37 MPa. The difference can be attributed to the higher content of the binding phase in the commercial metakaolin sample, whereas the MPSl sample contains partly high-temperature phases such as mullite. The higher pozzolanic activity of the commercial metakaolin resulted in increased reactivity, as reflected by the shorter setting time of 195 minutes compared to 255 minutes for the second sample. The addition of chamotte aggregate improved the mechanical properties by reducing shrinkage and cracking. Sodium water glass activated geopolymers exhibited higher strength than potassium activator, in accordance with the literature. The reasons for this are as follows: NaOH has a greater ability to liberate silicate and aluminate monomers during the initial stage of the geopolymerization process, when the aluminosilicate (metakaolin) particles are dissolved (Duxson et al. 2007, Li et al. 2025; Provis and Deventer 2009). The second reason is the smaller ionic radius of Na^+, which promotes the formation of a denser and more highly cross-linked aluminosilicate gel (Hounsi, et al. 2019). The best mechanical properties were achieved when sodium glass was used as an activator and alumina cement as a hardener, when the flexural strength was 15 MPa and the compressive strength was 85 MPa.

The results of refractoriness under load of selected geopolymer samples are shown in Fig. 7 (graph c). For comparison, the progression of the sample R was also included. The samples were not pre-fired. In the temperature range of approximately 100-200 °C, minor deformation occurred, probably caused by drying and hardening. As the temperature increased, a slight expansion of the samples was observed due to thermal expansion. In the temperature range of 850-1000 °C and 1150-1250 °C, more significant deformations of the samples occurred due to the effect of melting oxides CaO, K_2O and Na_2O and due to phase transformations. The sample with sodium-based activator was deformed at lower temperatures, in accordance with the literature (Zarębska et al. 2022). In contrast, the original MSCCh sample contained only 1.9 wt.% Na_2O, whereas the MPSlCh sample contained 3.8 wt.% K_2O, due to the differences in silicate modulus and solids content of the sodium and potassium water glasses (SWG and PWG). This highlights the strong fluxing effect of Na_2O. The CaO content in the MSCCh and MPSlCh samples is relatively low, at approximately 1 wt.%, and is therefore not expected to significantly reduce the refractory properties. Its primary source is the cement hardeners or slag, which are incorporated in a very small proportion of around 3 wt.%.

The main product of the geopolymer reaction is an alkaline aluminosilicate gel with a low degree of structural order, whose development is influenced, among other factors, by the K/Si, Na/Si, and Al/Si ratios. Short setting times and higher K/Si (or Na/Si) ratios lead to a less crystalline product (Shi et al. 2025). This effect is also attributed to the addition of slag or cement hardeners, which supply calcium that reacts with the dissolved silicate precipitates in the activator and accelerates the formation of the C-A-S-H gel and thus the geopolymerization (Kabirova et al. 2022). As a result of the relatively short setting times, the prepared geopolymers remain predominantly amorphous except for the high-temperature mullite and cristobalite phases present in the original FSD. The geopolymer structure, including

porosity, is influenced by the amount of mixing water, which was adjusted to achieve a similar consistency across geopolymer binders and mixtures, a key factor for material processing. In the case of metakaolin, water absorption is indirectly related to its reactivity, which supports the observation that a higher oil absorption value of the commercial metakaolin corresponds to higher strength of the geopolymer binder MefPSl compared to MPSl. The mixing water content also depends on the type of alkaline activator used. Potassium water glass exhibits higher stability in aqueous solutions due to the lower hydration energy of K+ compared to Na+, which allows for a higher solids concentration. Consequently, the potassium water glass used contained 54 wt.% dry matter, whereas the sodium water glass contained only 42 wt.% dry matter. The formation of N–A–S–H gel results in a greater proportion of bound water relative to P–A–S–H gel. The higher water-binding capacity may accelerate the transformation of free water into gel-bound water, leading to a reduction in the fluidity of fresh geopolymer pastes (Zhang et al. 2020).

The following table presents a comparison of the mechanical properties of the prepared geopolymer samples with examples reported in the literature. The obtained strengths are relatively high, particularly for the sample activated with sodium water glass. Aggregate, as well as other potential additives, appears to have a significant influence. For instance, several studies report that the addition of fibers leads to a significant increase in flexural strength.

Table 5. Comparison of results with literature data (Bezerra and Luz 2024; Albidah, et al. 2021; Mohmmad et al. 2023; Skyrianou et al. 2025; Kuenzel et al. 2014; Xu et al. 2025; Borçato et al. 2023; Latella et al. 2008; Li et al. 2022; Chairunnisa et al. 2024; Tippayasam et al. 2014; Zhang et al. 2023; Yang et al. 2022).

Title	Activator	σ_C (MPa)	σ_{FL} (MPa)
MSCCh	Na-based	84.6	15.0
Literature	Na-based	35.3–100.0	5.2–30.0
MPSlCh	K-based	41.2	11.9
Literature	K-based	30.3–80.0	6.7–13.1

4. Conclusions

Fly shale dust FSD mixed with water could be pelletized by extrusion through an adapter with circular meshes with a diameter of 9 mm. The key to creating cylindrical granules was to maintain a relatively narrow water content, when the mixture had the consistency of a ductile mass with lower plasticity. If the water content was low, the extruder could not push the mixture through the output adapter. Otherwise, the extruded mixture stuck together. The dried granulate contained particles in the range of approximately 0-10 mm, while the proportion of fine particles below 1.25 mm was 22%. Industrial-scale extrusion or pellet pressing could likely produce denser granules with lower porosity. The compressive strength of the dried mixture reached around 1 MPa. By firing granulate, it was possible to produce a refractory aggregate with a bulk density of 2180 kg/m^3, an absorbency of 4.1% and an apparent porosity of 9.0%. With the addition of alumina (RA sample), sintering occurred at a temperature 200-250 °C higher. At the same time, it exhibited a higher degree of mullitization during firing. This confirmed that the refractory properties of aggregates corresponded to their sintering activity (Liu et al. 2022). The material prepared in this study was comparable to lower quality commercial chamotte, but it still exhibits very good properties. Although it contained a slightly higher proportion of TiO_2, the material maintained a high refractoriness above 1670 °C, due to its high Al_2O_3 content and low alkali oxide content.

By firing the FSD granulate at a temperature of 650 °C, it was possible to increase the pozzolanic activity of the powder from the original 172 mg/g to 476 mg/g. For comparison, the commercial sample of metakaolin had a higher pozzolanic activity of 932 mg/g. The prepared pozzolanic material has been successfully tested for the production of geopolymers, achieving a flexural strength of 15 MPa and a compressive strength of 85 MPa. Therefore, it can be considered suitable as an active additive in construction materials. The addition of metakaolin to cement typically ranges between 5 and 15%, while in special applications it may reach up to 25%. Fillers are commonly added at levels of up to 5%. The metakaolin prepared in this study contains a partial filler component, primarily the high-temperature phase mullite. Therefore, its addition into concrete mixtures is optimum, as both its pozzolanic activity and filler effect can be utilized. In the case of cement itself, a lower addition should be considered, with expected levels of approximately 5–8%, which also contributes to a reduction in CO_2 emissions associated with cement production.

Although the products from both studied processes exhibit lower quality than commercially available variants, they still represent materials with high potential applications. Refractory aggregate could be used for the production of fireclay bricks or castables. Metakaolin could be added to concrete mixtures, serving both as a reactive component with cement and as a filler. Their technological production process involves standard operations such as granulation, drying, firing, and grinding. However, the critical factor in industrial scale will be the techno-economic analysis, which should consider reduced energy costs for input processing (crushing and grinding), increased costs for treatment (granulation), lower revenues due to slightly inferior product quality, and simultaneously lower landfill costs.

Acknowledgements

This research has previously been presented at SUROVINY 2023 held in Prague, Czechia, on May 17-18, 2023. Extended version of the research has been submitted to Challenge Journal of Concrete Research Letters and has been peer-reviewed prior to the publication.

Funding

The authors received no financial support for the research, authorship, and/or publication of this manuscript.

Conflict of Interest

The authors declare(s) no potential conflicts of interest with respect to the research, authorship, and/or publication of this manuscript.

Data Availability

The datasets generated and/or analyzed during the current study are not publicly available but are available from the corresponding author upon reasonable request.

AI Assistance

No AI-based tools were used in the preparation of this manuscript.

Author Contributions

All authors made substantial contributions to the conception and design of the study, acquisition of data, analysis and interpretation of data; drafted or critically revised the manuscript for important intellectual content; and approved the final version to be published.

REFERENCES

Abdelgader H, Amran M, Kurpińska M, Mosaberpanah M, Murali G, Fediuk R (2022). 10 - Cement kiln dust. *In*: *Ramezanianpour AA. Sustainable Concrete Made with Ashes and Dust from Different Sources.* Woodhead Publishing, Cambridge, United Kingdom, 451-479.

Aird P (2019). Deepwater Drilling. Gulf Professional Publishing, Oxford, United Kingdom.

Albidah A, Alghannam M, Abbas H (2021). Characteristics of metakaolin-based geopolymer concrete for different mix design parameters. *Journal of Material Research and Technology,* 10, 84-98.

Andrews A., Adam J, Gawu SK (2013). Development of fireclay aluminosilicate refractory from lithomargic clay deposits. *Ceramics International,* 39(1), 779-783.

Aziz I, Abdullah M, Yong H, Ming L, Hussin K, Azimi E (2015). A review on mechanical properties of geopolymer composites for high temperature application. *Key Engineering Materials,* 660, 34-38.

Bezerra B, Luz A (2024). High-alumina refractory castables bonded with metakaolin-based geopolymers prepared with different alkaline liquid reagents. *Ceramics International,* 50(11), 18628–18637.

Boateng A (2008). Rotary Kilns. Butterworth-Heinemann, Oxford, United Kingdom.

Bojanovský J, Máša V, Hudák I, Skryja P, Hopjan J (2022). Rotary kiln, a unit on the border of the process and energy industry—Current state and perspectives. *Sustainability,* 14(21), 13903.

Borçato AG, Thiesen M, Medeiros RA (2023). Mechanical properties of metakaolin-based geopolymers modified with different contents of quarry dust waste. *Construction and Building Materials,* 400, 132854.

Bucher R, Cyr M, Escadeillas G (2021). Performance-based evaluation of flash-metakaolin as cement replacement in marine structures – Case of chloride migration and corrosion. *Construction and Building Materials,* 267, 120926.

Chairunnisa N, Haryanti N, Nurwidayati R, Pratiwi A, Arnandha Y, Manik T, Suryajaya, Saputra Y, Hazizah N (2024). Characteristics of metakaolin-based geopolymers using bemban fiber additives. *Materials Science,* 11(4), 815-832.

Chakraborty A (2014). Phase Transformation of Kaolinite Clay. Springer India, New Delhi, India.

Cong P, Cheng Y (2021). Advances in geopolymer materials: A comprehensive review. *Journal of Traffic and Transportation Engineering,* 8(3), 283-314.

Debnath N, Boga S, Singh A, Majhi M, Singh V (2022). Fabrication of low to high duty fireclay refractory bricks from lignite fly ash. *Ceramics International,* 48(9), 12152-12160.

Djangang C, Elimbi A, Melo UC, Lecomte GL, Nkoumbou C, Soro J, Bonnet JP, Blanchart P, Njopwouoy D (2008). Sintering of clay-chamotte ceramic composites for refractory bricks. *Ceramics International,* 34(5), 1207-1213.

Duxson P, Fernández-Jiménez A, Provis JL, Lukey GC, Palomo A, Deventer JS (2007). Geopolymer technology: the current state of the art. *Journal of Materials Science,* 42, 2917–2933.

EN 993-1 (2018). Methods of test for dense shaped refractory products – Part 1: Determination of bulk density, apparent porosity and true porosity. European Committee for Standardization, Brussels, Belgium.

Hounsi AD, Lecomte-Nana G, Djétéli G, Blanchart P, Alowanou D, Kpelou P, Napo K, Tchangbédji G, Praisler M (2019). How does Na, K alkali metal concentration change the early age structural characteristic of kaolin-based geopolymers. *Ceramics International,* 40(7), 8953-8962.

Jala S, Sharma P (2019). Effect of cement kiln dust and RBI grade 81 on engineering properties of plastic clay. *Proceedings of the International Conference on Environmental Geotechnology, Recycled Waste Materials and Sustainable Engineering.* Singapore, 37-49.

Jia F, Su J, Song S (2015). Can natural muscovite be expanded? *Colloids and Surfaces A: Physicochemical and Engineering Aspects,* 471, 19-25.

Kabirova A, Uysal M, Hüsem M, Aygörmez Y, Dehghanpour H, Pul S, Canpolat O (2022). Physical and mechanical properties of metakaolin-based geopolymer mortars containing various waste powders. *European Journal of Environmental and Civil Engineering,* 27(2), 437-456.

Kaminskas R, Savickaite B (2023). Expanded clay production waste as supplementary cementitious material. *Sustainability,* 15(15), 11850.

Khan I, Xu T, Castel A, Gilbert RI, Babaee M (2019). Risk of early age cracking in geopolymer concrete due to restrained shrinkage. *Construction and Building Materials,* 229, 116840.

Kuenzel C, Li L, Vandeperre L, Boccaccini AR, Cheeseman CR (2014). Influence of sand on the mechanical properties of metakaolin geopolymers. *Construction and Building Materials,* 66, 442-446.

Lam M, Nguyen D, Nguyen D (2021). Potential use of clay brick waste powder and ceramic waste aggregate. *Construction and Building Materials,* 313, 125516.

Latella BA, Perera D, Durce D, Mehrtens EG, Davis J (2008). Mechanical Properties of Metakaolin-Based Geopolymers with Molar Ratios of Si/Al≈2 and Na/Al≈1. *Journal of Materials Science,* 43, 2693-2699.

Li L, Boumediene N, Follet C, Yang B, Promis G (2025). A review study: The effect of activator type on the compressive basic creep of alkali-activated materials under autogenous condition. *Results in Engineering,* 29, 108831.

Li Q, Chen S, Zhang Y, Hu Y, Wang Q, Zhou Q, Yan Y, Liu Y, Yan D (2022). Effect of curing temperature on high-strength metakaolin-based geopolymer composite (HMGC) with quartz powder and steel fibers. *Materials,* 15(11), 3958.

Liu Y, Xu L, Chen M, Zhang D (2022). Effects of andalusite and kyanite addition on the microstructure, thermo-mechanical properties and corrosion resistance of ultralow-cement bauxite-corundum castables. *Ceramics International,* 48(10), 14141-14150.

Lopes A, Lopes S, Pinto M (2023). Flexural stiffness and structural behavior of alkali-activated metakaolin faced with cement-based beams. *Journal of Building Engineering,* 76, 18.

Malaiškiene J, Antonovič V, Boris R, Stonys R (2022). Improving the physical and mechanical properties and alkali resistance of fireclay-based castables by modifying their structure with SiO2 sol. *Ceramics International,* 48(15), 22534-22544.

Mohmmad S, Shakor P, Muhammad J, Hasan M, Karakouzian M (2023). Sustainable alternatives to cement: Synthesizing metakaolin-based geopolymer concrete using nano-silica. *Construction materials,* 3(3), 276-286.

Muhammed N, Olayiwola T, Elkatatny S (2021). A review on clay chemistry, characterization and shale inhibitors for water-based drilling fluids. *Journal of Petroleum Science and Engineering,* 206, 109043.

NF P18-513 (2012). Addition for concrete - Metakaolin - Specifications and conformity criteria. AFNOR, Paris, France.

Özkılıç YO, Başaran B, Aksoylu C, Karalar M, Martins HM (2023). Mechanical behavior in terms of shear and bending performance of reinforced concrete beam using waste fire clay as replacement of aggregate. *Case Studies in Construction Materials,* 18, e02104.

Padmalosan P, Vanitha S, Kumar VS, Anish M, Tiwari R, Dhapekar NK, Yadav AS (2023). An investigation on the use of waste materials from industrial processes in clay brick production. *Materials Today: Proceedings,* 67, 1-4.

Panesar D (2019). Supplementary cementing materials. *In: Mindess S. Developments in the Formulation and Reinforcement of Concrete (Second Edition).* Woodhead Publishing, Cambridge, United Kingdom, 55-85.

Pillay D, Olalusi O, Kiliswa M, Awoyera P, Kolawole J, Babafemi A (2021). Engineering performance of metakaolin based concrete. *Cleaner Engineering and Technology,* 6, 100383.

Provis JL, Bernal S (2014). Geopolymers and related alkali-activated materials. *Annual Review of Materials Research,* 44, 299-327.

Provis JL, Deventer JS (2009). Geopolymers, Structures, Processing, Properties and Industrial Applications. Woodhead Publishing, Cambridge, United Kingdom.

Rasekh, H., Joshaghani, A., Jahandari, S., Aslani, F., & Ghodrat, M. (2020). Rheology and workability of SCC. *In: Siddique R. Self-Compacting Concrete: Materials, Properties and Applications.* Woodhead Publishing, Cambridge, United Kingdom, 31-63.

Riaz M, Khitab A, Ahmed S (2022). Evaluation of sustainable clay bricks incorporating Brick Kiln Dust. *Journal of Building Engineering,* 24,100725.

Rimstidt JD, Chermak JA, Schreiber ME (2017). Processes that control mineral and element abundances in shales. *Earth-Science Reviews,* 171, 383-399.

Saleh A, Abdel-Gawwad HA, EL-Moghny, MGA, El-Deab MS (2021). The sustainable utilization of weathered cement kiln dust in the cleaner production of alkali activated binder incorporating glass sludge. *Construction and Building Materials,* 300, 124308.

Salehi M, Salem A (2008). Effect of moisture content on extrusion process of kaolinitic–illitic clay in manufacturing of ceramic Raschig ring. *Journal of Materials Processing Technology,* 200(1-3), 232-237.

Samadi A, Gao L, Kong L, Orooji Y, Zhao S (2022). Waste-derived low-cost ceramic membranes for water treatment: Opportunities, challenges and future directions. *Resources, Conservation and Recycling,* 185, 106497.

Sheng JJ (2020). Chapter One - Introduction to shale and tight reservoirs. *In: Alfarge D, Wei M, Bai B, Chen Z. Enhanced Oil Recovery in Shale and Tight Reservoirs.* Gulf Professional Publishing, Cambridge, United Kingdom, 1-6.

Shi C, Liu Y, Qin L, Ghafoor MT, Zhang Z (2025). Time-dependent evolution of the microstructural characteristics of C-A-S-H and N-A-S-H gels with various Ca/Si and Al/Si ratios. *Construction and Building Materials,* 502, 144408.

Skyrianou I, Koutas LN, Papakonstantinou CG (2025). Metakaolin-based geopolymer mortars: Influence of mix design on mechanical properties and durability. *Construction and Building Materials,* 490, 142526.

Stokes JL (2024). β-Cristobalite thermal expansion and stability in environmental barrier coating systems. *Journal of the American Ceramic Society,* 108(2), e20214.

Tippayasam C, Balyore P, Thavorniti P, Kamseu E, Leonelli C, Chindaprasirt P, Chaysuwan D (2014). Potassium alkali concentration and heat treatment affected metakaolin-based geopolymer. *Construction and Building Materials,* 104, 293-297.

Xu W, Briffaut M, Gay N, Shao J (2025). Experimental investigation on the physical and mechanical properties of metakaolin-based geopolymers: Effects of aging and confining pressure. *Applied Clay Science,* 276, 107910.

Yang J, Xu L, Wu H, Jin J, Liu L (2022). Microstructure and mechanical properties of metakaolin-based geopolymer composites containing high volume of spodumene tailings. *Applied Clay Science,* 218, 106412.

Zarębska K, Zabierowski P, Grzywacz MG, Czuma N, Baran P (2022). Fly ash-based geopolymers with refractoriness properties. *Clean Technologies and Environmental Policy,* 24, 2161-2175.

Zhang DW, Zhao KF, Xie F, Li H, Wang D (2020). Effect of water-binding ability of amorphous gel on the rheology of geopolymer fresh pastes with the different NaOH content at the early age. *Construction and Building Materials,* 261, 120529.

Zhang Y, Chen J, Xia J (2023). Compressive strength and chloride resistance of slag/metakaolin-based ultra-high-performance geopolymer concrete. *Materials,* 16(1), 181.

Zheng J, Zhao L, Du W (2022). Hybrid model of a cement rotary kiln using an improved attention-based recurrent neural network. *ISA Transactions,* 129, 631-643.